



Full Length Article

Optimization of Measurement Conditions to Quantify PGR5-Dependent Cyclic Electron Flow Rate in Mulberry and Tobacco Leaves

Yan-Hui Che, Hong-Rui Wang, Yue Wang and Guang-Yu Sun*

Key Laboratory of Saline-alkali Vegetation Ecology Restoration, Ministry of Education, College of Life Science, Northeast Forestry University, Harbin 150040, China

*For correspondence: sungy@nefu.edu.cn

Received 25 March 2020; Accepted 13 August 2020; Published 10 October 2020

Abstract

Cyclic electron flow (CEF) around photosystem I (PSI) plays an important role in supplying the ATP shortfall for the Calvin-Benson cycle, as well as supplementing proton gradient that underpins non-photochemical quenching for photoprotection of PSII. Methods on its quantification in vitro were widely described in vitro in chloroplasts or thylakoids isolated from plant leaves, but its quantification in vivo is still very difficult. Here we proposed a new method to quantify in vivo CEF rate. The $P700^+$ signals under different oxidation times at given light intensity and the maximum $P700^+$ signal (P_m) were measured using mulberry as experimental material, and the ratio of $P700^+$ signal to P_m was used to quantify the magnitude of PGR5-dependent cyclic electron flow. The responsive model and simulation equation, taking the time and intensity of the far-red light on and off as independent variables and $P700^+$ signal intensity as dependent variables, were established to estimate accurately CEF rate in leaves of mulberry. This method has been verified in leaves of tobacco plants. © 2020 Friends Science Publishers

Keywords: Cyclic electron flow; PSI maximum fluorescence signal; Photosystem; Fitting equation

Introduction

During photosynthesis, the photoreaction drives the cyclic electron transport of photosystem I (PSI) (Evans and Vogelmann 2010). The transference of photosynthetic electrons into cyclic electron transporters is called CEF. (Takahashi *et al.* 2009; Huang *et al.* 2015). The PSI cyclic electron transfer has two known pathways: The main pathway depends on proton gradient regulatory protein 5 (PGR5) (Munekage *et al.* 2002), while the secondary pathway is regulated by a chloroplast NADH dehydrogenase-like (NDH) complex (Eva *et al.* 2000). Compared with linear electron transfer, cyclic electron transport only requires PSI to accompany cytochrome b_6/f complex during photochemical reactions. This is then accompanied by proton transfer from the stroma to the lumen on the thylakoid membrane (Okegawa *et al.* 2007), which generates a proton gradient (Δ pH) (Shikanai 2007) across the thylakoid membrane and drives ATP synthesis; however, this pathway does not produce NADPH is present. This mechanism has long been found in light-energy utilizing eukaryotes and enables plants to cope with fluctuating and high-light environment (Munekage *et al.* 2004; Tikkanen *et al.* 2010; Sugimoto *et al.* 2013; Kono *et al.* 2014).

Currently, the role of the PGR5-dependent CEF in photosynthesis regulation has been widely studied. And it is generally acknowledged that PGR5-dependent CEF is the main pathway of the photosynthetic CEF. However, its magnitude is difficult to be accurately determined. A common method to quantify the PGR5 CEF is in fact measuring the re-reduction rate of $P700^+$ after illuminating leaves with weak red light (Munekage *et al.* 2004; Okegawa *et al.* 2007). However, this method has several disadvantages: 1) In leaves adapted to weak far-red/direct red-light exposure, $P700^+$ will undergo incomplete oxidation, thus not reaching its full potential; 2) PSI of the thylakoid might not be sufficiently activated under weak far-red light. For example, when a leaf is illuminated from the adaxial side, upper chloroplasts are light saturated, while lower chloroplasts are not (Terashima *et al.* 2009). Previous studies demonstrated that the re-oxidation rate of $P700^+$ obtained by direct light was lower than that obtained by first dark adaptation and then light (Sergi *et al.* 2005). This is the reason why far red light can fully oxidize PSI but not PSII. After dark adaptation, PSI can be fully oxidized under far-red light. When the far red light is tuned off, PSII only transfer few electrons to reduce $P700^+$, therefore the $P700^+$ reduction is mainly caused by CEF (Burrows *et al.* 1998).

Mulberry has been widely concerned in recent years.

Mulberry leaves can eliminate bacteria in the body and play an anti-inflammatory and bactericidal role and so on. The signal amplitude of P700 determined by M-PEA can be evaluated to determine the PGR5 CEF size. However, most of the experiments conducted in China and abroad directly observed the P700 oxidation level after illumination with far-red light (Fan *et al.* 2002; Munekage *et al.* 2008; Suorsa *et al.* 2012; Sugimoto *et al.* 2013). Woody plants (mulberry) were used as material and the method was improved based on the work of predecessors (Zhong *et al.* 2018). Before exposing plants to far red-light radiation, plants were dark adapted for 30 min. we determine the influence of different intensities of far red light and different exposure durations on the PGR5 cyclic electron transport. At the same time, the mathematical model and 3D graphics were established, the response surface was observed, and the experiment was optimized, to acquire a suitable optimization method for the determination of the PGR5 CEF around PSI. This will provide information for future evaluation of mulberry photosynthetic efficiency under stress.

Materials and Methods

Plant material and culture conditions

Mulberry plants (*Morus alba*, one-year-old seedlings) were used as experimental materials, and were provided by the sericulture research institute of Heilongjiang province. Mulberry seedlings were cultured in a mixture of lime and vermiculite (volume ratio of 2:1) and were transplanted to the mixing matrix when plants had a length of 50 cm and growth chambers with the following environmental conditions: 12 h photoperiod, temperature of 25°C/20°C (day/night) and PPFD of 600 $\mu\text{mol m}^{-2} \text{s}^{-1}$.

Determination and Model of the P700 absorbance change

A light-intensity-time dependent experiment was determined by a plant efficiency meter M-PEA (Hansatech, Norfolk, U.K.) and conducted to study the PGR5-dependent CEF: the intensity of far red light was 20, 50 and 80%, which were named LFR, MFR and HFR, respectively (the intensity of 100% is 1000 $\mu\text{mol m}^{-2} \text{s}^{-1}$ $\lambda = 735 \pm 15 \text{ nm}$). The exposure times of far-red light were 20 s, 40 s, 60 s, 80 s, and 100 s. The time setting of the second curve is identical to that of the first curve. The data in the light intensity and time free combination analysis were manually quantified (Zhong *et al.* 2018).

The redox kinetic curve of P700⁺ was divided into four steps: 1) after dark adaptation of the leaves for 30 min, plants were irradiated with far-red light to oxidize P700. This process only used a proton gradient as the main driving force to promote the formation of ATP; therefore, the P700 signal would significantly decrease; 2) the far-red light exposure was stopped, and the P700 signal was restored to

the level in dark due to the electron input from CEF. 3) irradiate plants with far-red light with the same intensity that was used during the first stage; 4) finally, a 1 s-saturated far-red light exposure (100%, maximum intensity 1000 $\mu\text{mol m}^{-2} \text{s}^{-1}$ $\lambda = 735 \pm 15 \text{ nm}$) was used to saturate plants and an effective supplementary light (white light, 5000 $\mu\text{mol m}^{-2} \text{s}^{-1}$) was turned on synchronously to determine the maximum signal (Pm) of P700 (Fig. 1A). The second section is the reduction degree of P700⁺, which can be used as a qualitative representation of the size of CEF in the PGR5 pathway. To avoid problems caused by the light absorbance difference among different species and varieties, the ratio of the reduction degree of P700⁺ and Pm was used to characterize the PGR5 cyclic electron transport. Fig. 1B shows an enlarged model of the P700⁺ reduction degree /Pm.

Equation model and student-dependent residuals of the relationship between PGR5-dependent CEF and each variable

Dark interval time between far-red illuminations at step two (20 s, 40 s, 60 s, 80 s, 100 s), far-red light illumination time at step one (20 s, 40 s, 60 s, 80 s, 100 s), far red-light intensity at step one (20%, 50%, 80%) are independent variables, and CEF is the dependent variable. Box-behnen module is used to screen out reasonable models. The student-dependent residua are automatically given by the software.

Methods of data processing and statistics

SPSS (22.0) software was used for the statistical analysis of the data. Charts were plotted with Excel (2016) and Origin 9.1 (Origin Lab., US) was adopted to visualize a three-dimensional (3D) plot of the light intensity and exposure time. One-way analysis of variance (ANOVA) and least significant difference (LSD) were used to compare the differences between groups. Box-Behnken of Design-Expert 8.0.6 Trian (Stat-Ease, U.S.) was used to simulate both the response surface and equation, and to optimize the experimental scheme (Liu *et al.* 2011).

Results

Effects of different exposure time on signal oxidation of mulberry leaf P700

Fig. 2A shows that the P700⁺ reduction degree under LFR (20%) oxidation is highest, followed by MFR (50%) and HFR (80%). When far-red light was turned off after 20 s, 40 s, 60 s, 80 s, 100 s, respectively, LFR was higher than MFR and HFR. As shown in Fig. 2B, LFR exposure for 40 s and the time to turn off the far-red light were not significantly related to the reduction degree of P700⁺, and the difference between each point was not significant. HFR exposure for 40 s showed no significant difference between each point;

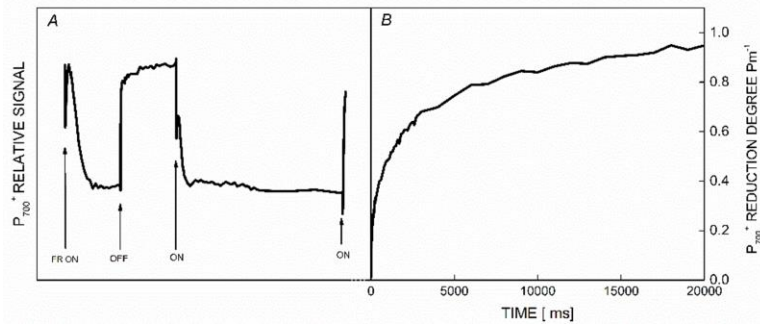


Fig. 1 a): Kinetic curve of P700⁺ REDOX; **b)** Dark reduction kinetics curves of P700⁺ with far red light off.

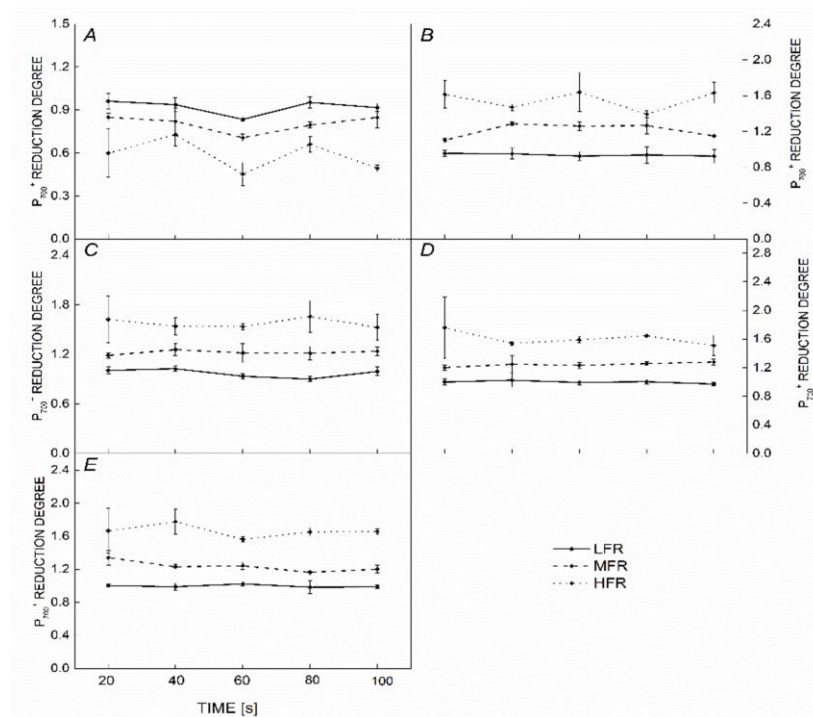


Fig. 2: Effects of different closing time and different percentage light intensity on P700 signals in 20 s, 40 s, 60 s, 80 s and 100 s (Correspond to Figure A, B, C, D and E respectively) far-red light irradiation in the oxidation stage. Where LFR is low intensity far-red light (20%); MFR is medium intensity far-red light (50%); HFR is higher intensity far-red light (80%). The time nodes of turning off the action light were divided into 20 s, 40 s, 60 s, 80 s and 100 s. Data are means with error bars indicating SD (n = 3 or 4). Different letters indicate significant differences ($P < 0.05$) and very different ($P < 0.01$) among the treatments and refer to each subset of data within each sampling date. The same below

however, the reduction degree of P700⁺ fluctuated. MFR exposure for 40 s, the reduction degree of P700⁺ increases first and then decreases. As shown in Fig. 2C, under irradiation for 60 s with different intensities of the far-red light, the light intensity curves of each intensity tended to flatten out and the difference between each point was not significant with increasing closing time. The HFR curve showed a large fluctuation range, with the highest reduction degree of P700⁺, followed by MFR and the lowest was found for LFR. The curves of far-red light irradiation for durations of 80 s and 60 s were similar. While the MFR and LFR curves tended to flatten, HFR fluctuated (Fig. 2D). Under HFR exposure, the P700 signal intensity was

significantly higher than that of the other intensities. The result of far red-light irradiation time of 100 s is the same (Fig. 2E).

The optimal combination of the P700⁺ reduction degree under different oxidation times

According to the presented results, the following combinations of maximum P700⁺ reduction degree were obtained: 20 s LFR irradiation, followed by darkness for 80 s (group 1); 40 s HFR irradiation, followed by darkness for 60 s (group 2); 60 s HFR irradiation, followed by darkness for 80 s (group 3); 80 s HFR irradiation, followed by

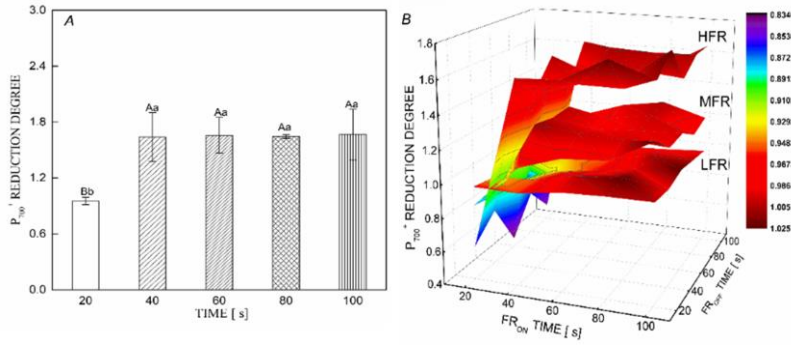


Fig. 3 a): Comparison of the maximum P700+ reduction degree obtained by the far-red light irradiated at different seconds in the first stage; the time nodes of irradiated far-red light were divided into 20 s, 40 s, 60 s, 80 s and 100 s. **b)** Time - light intensity dependent 3D surface view. The redder the color, the greater the value. FR_{ON}: Time to turn on the far-red light; FR_{OFF}: Turn off the time of far-red light; HFR: high intensity far-red light; MFR: medium intensity far-red light; LFR: low intensity far-red light. The same to below

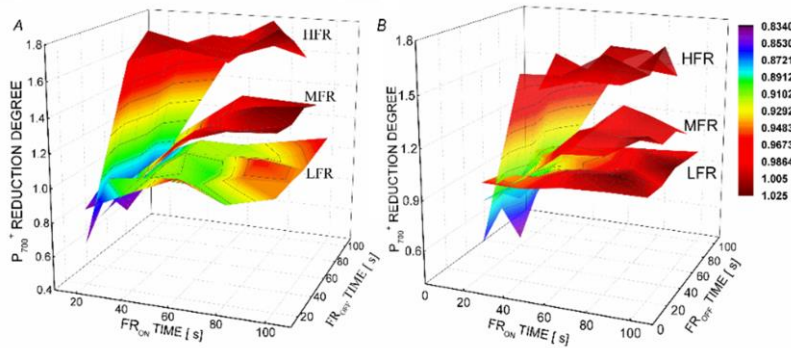


Fig. 4 a): Tobacco light intensity-time dependent test 3D layer; **b)** Mulberry light intensity - time dependent test 3D layer

darkness for 80 s (group 4); 100 s HFR irradiation, followed by darkness for 20 s (group 5) (Fig. 3A). The reduction degree of P700⁺ was smallest for group 1, while those of groups 2–5 were higher compared with group 1. The maximum combinations of the last four groups were all exposed to HFR, and no significant differences were found between them. The 3D surface diagram (Fig. 3B), which was simulated for each data point, shows that PGR5-dependent CEF under HFR was the smallest, while LFR achieved the largest before and around 20 s of the far-red light exposure; MFR was the largest.

Relationship model between PGR5-dependent CEF and each variable

Table S10 and Table S9 (supplementary material) show the ANOVA comparison between the PGR5 CEF and various fitting models with different parameters obtained by Design-Expert 8.0.6 Trian. Table S8 (supplementary material) shows the results of the confidence analysis of the quadratic model. The mean square and test results of variance analysis of different models in Table S10 indicate that the fitting effect of the quadratic equation model is recommend. Table S9 compares the complex correlation coefficients and the

results of the mean square error and folk square difference of each polynomial model that can be fitted. The result indicated the quadratic polynomial model as optimal. Table S8 shows the results of the confidence analysis of Design-Expert 8.0.6 Trian on the quadratic polynomial model and various influencing factors of the model. The results showed that the effect of fitting experimental data by the quadratic polynomial model is significant. Furthermore, the interaction between far-red light and light intensity among its parameters had the highest influence on PGR5 CEF. Under the interaction of all three factors, their order of influence on CEF followed: (open far-red light time * light intensity) > (open far-red light time * close far-red light time) > (close far-red light time * light intensity). From the perspective of a single factor, light intensity had the strongest impact on CEF.

Quadratic equation model and student-dependent residuals of the relationship between PGR5-dependent CEF and each variable

Equations (1) and (2) present the quadratic equation models of PGR5-dependent CEF. Each factor is expressed in factor code form and actual factor value form. Fig. 2s

(Supplementary Material) shows the student-oriented residual distribution of the fitting model, which shows that 97% of the points of the residual are distributed between -2 and 2, and lie almost on a straight line; consequently, the model achieved a good fit.

Final equation in terms of coded factors

$$\text{CEF} = +1.26 + 0.34 * A - 0.029 * B + 0.36 * C - 0.010 * A * B + 0.49 * A * C - 0.025 * B * C - 0.52 * A^2 + 0.020 * B^2 + 0.10 * C^2 \quad (1)$$

Final equation in terms of actual factors

$$\text{CEF} = +0.63972 + 0.015065 * A - 5.54996E - 004 * B - 0.61595 * C - 2.91266E - 006 * A * B + 0.016216 * A * C - 8.46677E - 004 * B * C - 1.44820E - 004 * A^2 + 5.62985E - 006 * B^2 + 0.41330 * C^2 \quad (2)$$

Where A: Time when FR was turned on; B: Time the FR was turned off (Dark time after turning off far-red light); C: The intensity of exposure to far-red light.

Experimental scheme optimization

Based on the analysis of the experimental results and model fitting, the experimental parameters were further optimized by using Design-Expert 8.0.6 Trian. The optimal scheme for the value of each parameter was thus obtained under the condition of the optimum CEF. Table S11 (supplementary material) shows the optimal scheme to obtain the optimum CEF. According to the optimization results, the best CEF is obtained when HFR is turned on for 97 s and turned off for 20 s, which is consistent with the optimal results in the experimental data.

Discussion

Cyclic electron transport around PSI remains one of the mysteries of photosynthesis. An important reason for the existence of this problem is that it is difficult to directly measure because the cycle has no net electron flow (Zhang *et al.* 2018). As an index, the P700⁺ level is direct and sensitive and measures the capability of receiving electrons in PSI. Under far-red light irradiation, the fast components of the P700⁺ decay are derived from cyclic electron transport (PGR5-dependent pathway). It has been shown that *Arabidopsis* mutants without PGR5 exhibit responses to high light levels (Nandha *et al.* 2007; DalCorso *et al.* 2008; Okegawa *et al.* 2010; Tikkanen *et al.* 2014), fluctuating light (Tikkanen *et al.* 2010), high temperature (Zhang and Sharkey 2009) and low CO₂ concentration (Munekage *et al.* 2008); hence, the CEF of the PGR5 pathway is particularly important. Depending on the PGR5 PSI, CEF is crucial for the acidification around the thylakoid lumen. Okegawa *et al.* (2007) used transgenic mutants and reported that overexpression of the PGR5 protein led to a delayed development of plant chloroplasts. Suorsa *et al.* (2012) showed that inhibition of

the PGR5 gene expression increased the intracavity pH, which interfered with the down-regulation of the Cyt b₆/f complex, thus resulting in the accumulation of excessive electrons in PSI, which in turn resulted in a reduction of P700.

According to prior research, on the basis of chlorophyll, the chloroplast at the bottom of leaf absorbs about 10–20% of the green light ($\lambda = 530 \pm 15$ nm) that is absorbed by the green leaves at the top (Fan *et al.* 2002), however, the fraction is much smaller for strongly absorbed wavelengths, such as red and blue (Katsumi 1976; Fan *et al.* 2002). This is consistent with the obtained experimental results (Fig. 2). To further stimulate the photosystem in the lower chloroplasts, the irradiation time has to be extended or the light intensity increased. The far-red light treatment is more irradiating and can therefore increase the content of chlorophyll b in the leaves. The antenna pigment chlorophyll b promotes the absorption and transmission of light energy, which can improve the net photosynthetic rate, and exerts a positive impact on photosynthesis (Cheng *et al.* 2018).

The experimental results suggested that after HFR irradiation of the leaves, the CEF was significantly higher than that of MFR and LFR. Because P700 oxidation accumulates numerous electrons, these can immediately be used for CEF after turning off the far-red light. At that moment, P700 is rapidly reduced and can reach a high level within a short period of time.

The equation model between CEF and light intensity time suggested by Design-Expert software is a quadratic mathematical equation. To test the fitting degree of this equation, the following diagnosis is necessary (eg: normal probability plot of the studentized residuals to test for normality of residuals). The diagnostic results showed that all model statistics and diagnostic graphs were satisfactory, and can therefore be used as the determination equation of the mulberry PGR5-dependent CEF.

Design-Expert software was used for the optimization process to identify the optimal combination of factors (Liu *et al.* 2011). Both response factor and process input factor remained within the scope of the requirements. In this experiment, the digital optimization method was used to optimize the equation by selecting the expected target of each factor and response. CEF was set to the condition that the maximum is the optimal combination. The simulated results showed that the maximum CEF per unit Pm can be obtained by turning the light off for 20 s after 97 s of far-red light irradiation. This is almost consistent with the results obtained by the intensity-time dependent test.

To test the effectiveness of this method in different plants, the model plant tobacco was used. Most of the times and light intensities were selected to determine the reduction degree of P700⁺ (supplementary data Tables S1–S3), origin 9.1 and Design-Expert 8.0.6 Trian were used to simulate 3D layers (Fig. 4A) and surface equations (Formula (3), please see below), respectively. To control

the variables used to explore the consistency of the results measured by this method between mulberry and tobacco, the experimental data was selected that was consistent with the results of mulberry and tobacco. The 3D layer (Fig. 4B) was repeated as was the surface equation {Formula (3)}. Fig. 4 shows that the trend of the tobacco 3D layer is consistent with that of the mulberry 3D layer, namely $HFR > MFR > LFR$. Formulas (3) and (4) represent the curved surface equations of tobacco and mulberry, respectively, and the coding factor equation coefficient of both was used for significance analysis in SPSS22.0 (Table 12s, supplementary materials). Furthermore, a comprehensive analysis of the tobacco data was conducted with Design-Expert. Supplementary data Tables S4–S6 showed that the tobacco equation was a quadratic polynomial simulation equation with good simulation effect (Fig. 1s), and the optimal combination was consistent with the mulberry experiment (Table S7). These results showed that the simple correlation coefficient between mulberry and tobacco was 0.952, indicating a strong positive correlation between them, which testifies the feasibility of this method for tobacco. In conclusion, the experimental method can be applied for the determination of the PGR5 cyclic electron transport between different plants.

Final equation in terms of actual factors for tobacco

$$CEF = + 0.57355 + 0.016740 * A - 5.42860E - 004B - 0.81237 * C - 3.76860E - 006 * AB + 0.014717 * A * C - 1.83021E - 003 * B * C - 1.44382E - 004 * A^2 + 1.43193E - 005 * B^2 + 1.00331 * C^2 \quad (3)$$

Final equation in terms of actual factors for mulberry

$$CEF = + 0.84479 + 0.011839 * A - 2.88142E - 003 * B - 1.12897 * C + 1.54509E - 006 * A * B + 0.016695 * A * C + 2.89548E - 004 * B * C - 1.19048E - 004 * A^2 + 2.02159E - 005 * B^2 + 0.85650 * C^2 \quad (4)$$

Conclusion

HFR can effectively stimulate PGR5-dependent cyclic electron flow. In addition, cyclic electron flow measured by the cyclic electron flow method per unit Pm can be used for the qualitative estimation of cyclic electron flow in different plants. The results of Design-Expert 8.0.6 Trian were consistent with the experimental results, and the optimal combination was: HFR turned on for 97 s, followed by turning off the far-red light for 20 s, and HFR irradiation for 60 s. Finally, far-red light of 100% ($1000 \mu\text{mol m}^{-2} \text{s}^{-1}$) and saturated light ($5000 \mu\text{mol m}^{-2} \text{s}^{-1}$) were used at the same time for 1 s. The mathematical model between PGR5 and switching far-red light time and light intensity can be expressed according to Equation (2).

Acknowledgments

This research was funded by the National Natural Science Foundation of China, grant number 31870373.

Author Contributions

Conceptualization, Y-H.C., and G-Y. S.; methodology, H-R.W., and Y.W.; software, H-R.W., and Y-H.C.; validation, Y.W.; investigation, Y-H.C.; data curation, Y-H.C., and H-R.W.; project administration, Y-H.C., and G-Y.S.; writing-original draft preparation, Y-H.C.; writing-review and editing, Y-H.C. and G-Y.S.; writing-discussion, Y-H.C., H-R.W., and G-Y.S.; funding acquisition, G-Y.S.; All authors have read and agreed to the published version of the manuscript

References

- Burrows PA, LA Sazanov, Z Svab, P Maliga, PJ Nixon (1998). Identification of a functional respiratory complex in chloroplasts through analysis of tobacco mutants containing disrupted plastid *ndh* genes. *EMBO J* 17:868–876
- Cheng YJ, JX Chen, ZL Wang, YF Fan, SY Chen, ZL Li, F Yang, WY Yang (2018). Effects of light intensity and light quality on morphological and photosynthetic characteristics of *Soybean* Seedlings. *Sci Agric Sin* 51:2655–2663
- DalCorso G, P Pesaresi, S Masiero, E Aseeva, D Schünemann, G Finazzi, P Joliot, R Barbato, D Leister (2008). A complex containing PGR1 and PGR5 is involved in the switch between linear and cyclic electron flow in *Arabidopsis*. *Cell* 132:273–285
- Eva M, OP Stefan, J Thierry, R Dominique, C Laurent, VH Gabor, TA Kavanagh, C Scha'fer, G Peltier, P Medgyesy (2000). Targeted inactivation of the plastid *ndhB* gene in tobacco results in an enhanced sensitivity of photosynthesis to moderate stomatal closure. *Plant Physiol* 123:1337–1349
- Evans JR, TC Vogelmann (2010). Profiles of C-14 fixation through spinach leaves in relation to light absorption and photosynthetic capacity. *Plant Cell Environ* 26:547–560
- Fan DY, Q Wang, M Li, GM Zhang, RF Gao (2002). The len effect of the epidermic cell layer of the leaf of euonymus *Japonicus T.* on the light gradients within leaf. *Acta Phytoecol Sin* 26:594–598
- Huang W, YJ Yang, H Hu, SB Zhang (2015). Different roles of cyclic electron flow around photosystem I under sub-saturating and saturating light intensities in tobacco leaves. *Front Plant Sci* 6; Article 923
- Katsumi I (1976). Action spectra for photosynthesis in higher plants. *Plant Cell Physiol* 17:355–365
- Kono M, K Noguchi, I Terashima (2014). Roles of the cyclic electron flow around PSI (CEF-PSI) and O₂-dependent alternative pathways in regulation of the photosynthetic electron flow in short-term fluctuating light in *Arabidopsis thaliana*. *Plant Cell Physiol* 55:990–1004
- Liu J, H Zhang, Y Shi (2011). Technology optimizing research on laser nonpenetration lap welding of stainless steel based on Design-Expert V7. *J Mech Eng* 47:52–60
- Munekage N, B Genty, G Peltier (2008). Effect of PGR5 impairment on photosynthesis and growth in *Arabidopsis thaliana*. *Plant Cell Physiol* 49:1688–1698
- Munekage Y, M Hashimoto, C Miyake, KI Tomizawa, T Endo, M Tasaka, T Shikanai (2004). Cyclic electron flow around photosystem I is essential for photosynthesis. *Nature* 429:579–582
- Munekage Y, M Hojo, J Meurer, T Endo, M Tasaka, T Shikanai (2002). PGR5 is involved in cyclic electron flow around photosystem I and is essential for photoprotection in *Arabidopsis*. *Cell* 110:361–371
- Nandha B, G Finazzi, P Joliot, S Hald, GN Johnson (2007). The role of PGR5 in the redox poisoning of photosynthetic electron transport. *Biochim Biophys Acta* 1767:1252–1259
- Okegawa Y, Y Kobayashi, T Shikanai (2010). Physiological links among alternative electron transport pathways that reduce and oxidize plastoquinone in *Arabidopsis*. *Plant J Cell Mol Biol* 63:458–468
- Okegawa Y, TA Long, M Iwano, S Takayama, Y Kobayashi, SF Covert, T Shikanai (2007). A balanced PGR5 level is required for chloroplast development and optimum operation of cyclic electron transport around photosystem I. *Plant Cell Physiol* 48:1462–1471

- Sergi MB, T Shikanai, K Asada (2005). Enhanced ferredoxin-dependent cyclic electron flow around photosystem I and alpha-tocopherol quinone accumulation in water-stressed ndhB-inactivated tobacco mutants. *Planta* 222:502–511
- Shikanai T (2007). Cyclic electron transport around photosystem I. *Annu Rev Plant Biol* 58:199–217
- Sugimoto K, Y Okegawa, A Tohri, TA Long, SF Covert, T Hisabori, T Shikanai (2013). A single amino acid alteration in PGR5 confers resistance to antimycin A in cyclic electron transport around PSI. *Plant Cell Physiol* 54:1525–1534
- Suorsa M, S Järvi, M Grieco, M Nurmi, M Pietrzykowska, M Rantala, S Kangasjärvi, V Paakkari, M Tikkanen, S Jansson, EM Aro (2012). PROTON GRADIENT REGULATION5 is essential for proper acclimation of *Arabidopsis* photosystem I to naturally and artificially fluctuating light conditions. *Plant Cell* 24:2934–2948
- Takahashi S, SE Milward, DY Fan, WS Chow, MR Badger (2009). How does cyclic electron flow alleviate photoinhibition in *Arabidopsis*. *Plant Physiol* 149:1560–1567
- Terashima I, T Fujita, T Inoue, WS Chow, R Oguchi (2009). Green light drives leaf photosynthesis more efficiently than red light in strong white light. *Plant Cell Physiol* 50:684–697
- Tikkanen M, NR Mekala, EM Aro (2014). Photosystem II photoinhibition-repair cycle protects Photosystem I from irreversible damage. *Biochim Biophys Acta* 1837:210–215
- Tikkanen M, M Grieco, S Kangasjärvi, EM Aro (2010). Thylakoid protein phosphorylation in higher plant chloroplasts optimizes electron transfer under fluctuating light. *Plant Physiol* 152:723–735
- Zhang MM, DY Fan, GY Sun, WS Chow (2018). Optimising the linear electron transport rate measured by chlorophyll a fluorescence to empirically match the gross rate of oxygen evolution in white light. *Funct Plant Biol* 45:1138–1148
- Zhang R, TD Sharkey (2009). Photosynthetic electron transport and proton flux under moderate heat stress. *Photosynth Res* 100:29–43
- Zhong X, YT Li, XK Che, QM Li (2018). The relationship between the activities of photosynthetic apparatus and the expressions of photosynthetic core proteins during the leaf expansion of *Cucumis sativus*. *Plant Physiol J* 54:1045–1054